Macromolecules
ARTICLE

Macromolecules **2010**, *43*, 511–517 **511**
DOI: 10.1021/ma901899m

Electromechanical Characterization of Polyelectrolyte Gels by Indentation

Katsiaryna Prudnikova[†,‡] **and Marcel Utz***[,†,‡,§]

[†]*Center for Microsystems for the Life Sciences,* [‡]*Department of Mechanical and Aerospace Engineering,* [§]*Department of Chemistry, and University of Virginia, Charlottesville, Virginia 22904*

Received August 26, 2009; Revised Manuscript Received October 23, 2009

ABSTRACT: We report an indentation method to quantify the electromechanical coupling in polyelectrolyte gels (PGs). PGs produce electric fields in response to mechanical stress and are therefore promising for mechanical sensor applications. The method exposes thin gel samples to well-defined pressure distributions through a spherical indentor, while the electrical response is measured with an array of platinum electrodes embedded in the support. A series of copolymer gels of acrylamide and acrylic acid were synthesized and equilibrated at a fixed pH, leading to samples with systematically varying spatial densities of both charged groups and cross-links. They were characterized by measuring the potential difference between the gel and the equilibrating solution (Donnan potential) as well as their electromechanical coupling through the indentation method. The electromechanical coupling was found to be proportional to the Donnan potential, while the latter is a universal function of the spatial density of ionizable groups in the gel, irrespective of the cross-link density.

Introduction

Polyelectrolyte gels (PGs) respond with an electrical potential difference to gradients in mechanical stress. The present work aims at quantifying this response in a well-defined and reproducible manner. Soft PGs are promising for applications as mechanical transducers with very low inherent stiffness. They are potentially biocompatible and could form the basis for incorporating tactile sensitivity into artificial skin systems. In the presence of a polar solvent, charged polymer systems tend to exhibit electromechanical effects.[1] For example, Nafion-type polymers, consisting of perfluorinated main chains with sulfonate or carboxylate groups on side chains, have received a substantial amount of interest as the basis of sensors and "artificial muscle" actuators.[2−4] These systems contain a small amount (a few percent) of water and are typically arranged in the form of thin films with electrodes electrochemically deposited on either side of the film. On the other hand, soft polyelectrolyte gels (PGs) consist of a cross-linked, charged polymer backbone, swollen in water with swelling ratios larger than 2. Ever since the first report of shape changes of poly(acrylic acid) gels in response to the application of an electrical potential by Tanaka et al.,[1] similar systems have been studied extensively due to their ability to deform in response to electrical and other stimuli, such as changes in pH, temperature, and salinity.[1,5−13]

Ultimately, it is clear that the response of charged polymer systems to electrical fields is due to the difference in mobility between the charges bound on the polymer backbone (usually anions) and the counterions (usually cations) which are free to diffuse in the solvent. However, there is still considerable debate on the details of the mechanism. In the case of soft PGs, it is currently assumed that exposure to electric fields leads to a redistribution of the free counterions, thus changing the osmotic pressure distribution in the system. This causes local changes in the swelling degree of the gel, resulting in macroscopic deformation.[14,15] By contrast, de Gennes has proposed an alternative description based on irreversible thermodynamics, noting the observed sensitivity of the mechanical response to the type of counterion present in the system.[7] This approach has been developed into a electrostress diffusion coupling model by Yamaue et al.[15]

Most of the available experimental data on electroactive polymers has been obtained by placing samples between electrodes, applying a voltage, and observing the resulting mechanical deformation. This setup is similar to the arrangement in electromechanical actuators. By contrast, the reverse effect, i.e., the electrical response to mechanical load, has only been studied semiquantitatively,[16] in spite of the direct relevance of such results to sensor applications. Moreover, the comparison of the experimental results from actuator-type setups with theoretical predictions is not trivial because complicated coupled transport equations for the solvent, charge, and polymer must be solved in a geometry that changes during the course of the experiment.

In the present contribution, we propose a quantitative test that is inspired by the application of charged polymer systems as sensors rather than actuators. A well-defined, nonhomogenous stress distribution is generated by indenting a planar polymer sample with a spherical indentor (Figure 1). The resulting electrical potential distribution is monitored via a system of concentric platinum electrodes that are fabricated into the support of the sample (Figure 1C). This setup provides quantitative data on the electromechanical coupling coefficient in a geometry that changes only very slightly during the course of the experiment.

In the present study, this method has been applied to a range of soft PGs consisting of copolymers of acrylic acid and acrylamide. The mole fraction of acrylic acid as well as the cross-link density has been varied systematically in order to produce gels with a range of densities of negative charge on the polymer backbone. The gels were equilibriated at a fixed pH and characterized in terms of their equilibrium swelling degree and the Donnan potential in the absence of mechanical load, in addition to electromechanical indentation experiment. As an alternative, the gels could have been neutralized to a specified degree by titration with sodium hydroxide. However, working at fixed pH

*To whom correspondence should be addressed.

Published on Web 11/16/2009

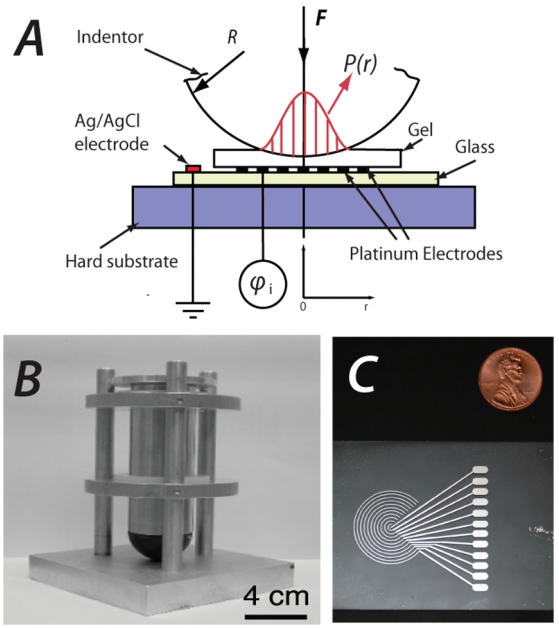

Figure 1. (A) Principle of the indentation experiment. (B) Indentor assembly. (C) Platinum electrode pattern.

seemed more relevant in view of future applications in physiological systems, which tend to be pH-buffered.

In a related study, reported separately, the streaming potential coefficient of the same type of gels was measured.[17] Together, these experiments have produced a consistent set of data that can be compared meaningfully to the predictions of existing theories of electromechanical coupling in charged polymer systems.

Background and Theory

The principle of the experiment is shown in Figure 1: A spherical indenter is pressed into a flat gel sample laying on a glass support which carries a pattern of concentric, circular Pt electrodes. The sample is immersed in a buffer solution (not shown in Figure 1), and a Ag/AgCl electrode in contact with the buffer is used as a reference point. The potential at each electrode is monitored using a high-impedance amplifier. In order to distinguish the signal from slow capacitive drift effects, the indenter load is modulated periodically, and a high-pass filter is applied to the signals. The mechanical contact of a hard sphere indenting a flat, elastic sample of finite thickness resting on a hard substrate is described by a modified Hertzian contact theory.[18] It predicts the following dependence of the pressure on the distance from the center:

$$P(r) = P_0\left(1 - \frac{r^2}{a^2}\right)^2 \qquad (1)$$

where $P_0 = 3(F/\pi a^2)$ is the pressure at the center of the contact circle. The radius of the contact circle is

$$a = \left(\frac{72FRh^3}{\pi E}\right)^{1/6} \qquad (2)$$

where R is the indenter radius and h and E denote the thickness and elastic modulus of the sample, respectively. Assuming a linear relationship between potential and pressure, the potential distribution in the gel sample is expected to follow the same functional profile as the pressure distribution.

The electromechanical interaction of charged polymers has been approached by both equilibrium and nonequilibrium thermodynamics. The equilibrium picture is based on the Donnan potential:[19] In contact with a polar solvent, the free counterions will diffuse out of the swollen gel until the corresponding gain in entropy is balanced by the electric potential difference between the inside and the outside of the gel. This leads to the formation of a charge double layer at the gel/liquid boundary. The magnitude of the Donnan potential depends on the density of dissociable groups in the gel and the osmotic pressure of the solvent. From this standpoint, applying local pressure to the gel is tantamount to an increase in osmotic pressure of the solvent, leading to a concomitant change in the Donnan potential.

An alternative viewpoint, based on nonequilibrium thermodynamics, has originally been suggested by de Gennes in the context of Nafion-type polymer actuators.[7] From this point of view, the electromechanical coupling is the result of the coupling between fluxes of charged species and the solvent, which are driven by the electrical potential and the osmotic pressure gradient, respectively. In the present contribution, we have quantified the electromechanical coupling in a range of PGs differing in concentration of ionizable groups and cross-link density. As explained in the following, we find a direct correlation between the Donnan potential and the electromechanical coupling coefficient, suggesting that the equilibrium approach provides an adequate picture for this type of gel.

Experimental Section

Materials. Acrylic acid (AA) (Aldrich, 99% purity) and acrylamide (AM) (Aldrich, 99+% purity, electrophoresis grade) were used as comonomers without purification. *N*,*N*′-Methylenebis(acrylamide) (nBisA) (Aldrich, 99% purity) and 2,2-dimethyl-2-phenylacetophenone (DMPA) (Aldrich, 99% purity) were used as received as cross-linker and photoinitiator, respectively. Potassium acid phtalate/methyl alchohol buffer solution pH 4.00 (Fisher) and dimethyl sulfoxide (DMSO) (Aldrich) were used as solvents for polymerization; potassium acid phtalate/sodium hydroxide buffer solution pH 5.00 (Fisher) was used for the swelling equilibration of the samples. Salinity of both buffer solutions was $C_s = 0.05$ M.

Gel Preparation. All copolymerizations were performed at an overall monomer concentration of 3.8 M and at constant pH 4.00, while the mole fraction of AA was varied between 0 and 1. At pH 4.00, the reactivity ratios of AA (r_{AA}) and AM (r_{AM}) monomers are equal and less than 1 ($r_{AA} \approx r_{AM} \approx 0.6 < 1$). This indicates preferential addition of the other monomer, which leads to an intermediate case between alternating and random copolymerization.[20]

In this way, three sequences of copolymers were created using different initial concentrations of nBisA: 22, 43, and 86 mM. The photoinitiator DMPA concentration was equal to 6.78 mM and was kept constant during all copolymerizations.

A solution of 0.0744 M DMPA in DMSO was prepared (solution A). AA, AM, and nBisA were dissolved in pH 4.00 buffer at a total monomer concentration of 4 M (solution B). The solutions were sonicated for 5 min and then combined to give 3.8 M overall monomer concentration. The resulting solution was degassed with dry nitrogen gas. The necessary amount of the mixture was poured in a square mold made of two microscope slides (Fisher) separated with PDMS spacers of 1.1 mm thickness. Polymerization was initiated by exposure to an UV lamp ($\lambda = 365$ nm) at room temperature for 10 min. The samples were then carefully removed from the mold and equilibrated in a buffer solution at pH 5.00, which was changed every 24 h until the samples reached constant weight (< 1% change in weight in 24 h). Typically, the samples reached equilibrium swelling in 3 days. Sample mass was monitored as a function of time by removing the gels periodically from the buffer solution and weighing on an analytical balance (Mettler Toledo)

after gentle drying with paper towels (Kimwipes, Kimberly and Clark, Inc.). Donnan potential measurements and indentation experiments were carried out after at least 1 week of equilibration.

Donnan Potential Measurements. Donnan potential measurements were carried out using Ag/AgCl electrodes prepared from Ag/AgCl wires (A-M Instruments). The Ag/AgCl wires were put into conical polypropylene pipet tips with an opening diameter of 0.2 mm, filled with 4 M KCl solution saturated with AgCl. The top of the tube was sealed to prevent loss of solvent due to evaporation. The potential difference between any two electrodes prepared in this way was less than 100 μV. The Donnan potential was measured between the gel sample and the surrounding solution. A reference Ag/AgCl electrode was kept in solution, while the surface of the gel sample was gently pressed with the working Ag/AgCl electrode. The resulting potential difference was recorded with a GAMRY Reference 600 potentiostat.

The potential difference was measured in three different locations of each gel sample. The potential was monitored for an acquisition time of 1 min, and the result was obtained by averaging the last 30 s.

Indentation. Concentric Pt electrodes were prepared by sputtering 100 nm of Pt onto a glass substrate (thickness 1 mm) using a negative photomask (Figure 1C). The width of the electrodes is 0.25 mm; the electrodes are separated by a radial distance 1 mm. The Pt electrodes were covered with a mask leaving only the central, circular area exposed to the sample.

The glass substrate with the electrodes was mounted on the bottom plate of the indentation device (Figure 1). The indenter axis was carefully aligned with the center of the electrodes. First, the sample was preloaded with the weight of the indenter itself ($F = 4.7$ N), and the system was allowed to stabilize for 20 min. Second, an additional force ($\Delta F = 3$ N) was applied at a frequency $f_0 = 0.025$ Hz, leading to a square-wave modulation between minimum and maximum values of the total applied force.

In order to calculate the pressure distribution in the sample, the contact radius was determined by placing a gel sample on a glass slide, indenting it with a hard spherical indenter (using the same indentation procedure), and monitoring the contact area with a digital camera placed beneath the glass slide.

Signal Acquisition. Acquisition of the potential signals was carried out during the indentation of the hydrogels to reveal the potential profile corresponding to an applied square-wave modulation of pressure. The potential signal was measured as potential V_i at the ith electrode with the respect to the grounded reference Ag/AgCl electrode. MOSFET operational amplifiers with high input impedance on the order of 10^{14} Ω were used. Two amplifier stages were combined to produce a voltage gain of 23 dB. The signal was sampled at 10kHz with a dynamic range of better than 16 bit.

Results and Discussion

Swelling Equilibrium. The swelling degree is defined as $Q = m_{sw}/m_0$, where m_{sw} is the mass of the fully equilibrated sample and m_0 is the total mass of the monomers used for its synthesis. The equilibrium swelling degrees were saturated with the respect to reaction time. No changes in equilibrium swelling were observed for the exposure times $t > 10$ min, indicating that maximum conversion rates were achieved at our preparation conditions.

Figure 2 shows the swelling degrees of poly(acrylamide-*co*-acrylic acid) gels prepared at three different initial concentrations of cross-linker $C_{nbisA} = 22$, 43, and 86 mM, after equilibration in pH 5 buffer. pH 5.00 buffer was used to ensure dissociation of acrylic acid groups (ionization degree $\alpha = 0.5$ for $pK_a = 5$)[21] and simultaneously maintain the swelling degrees reasonably low for practical handling of the gels.

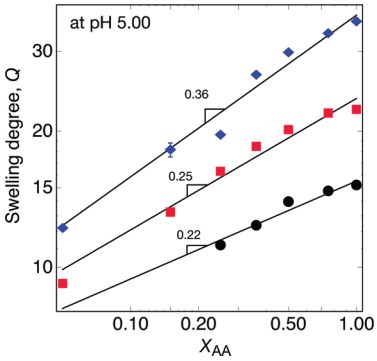

Figure 2. Double-logarithmic plot indicating different dependence of the swelling degree of PGs Q on the fraction of acrylic acid monomer at preparation X_{AA} for different initial concentrations of the cross-linker nBisA C_{nbisA}: black circles, $C_{nbisA} = 86$ mM; red squares, $C_{nbisA} = 43$ mM; blue rhombs, $C_{nbisA} = 22$ mM. Error bars correspond to 3σ, calculated from the swelling degrees of four samples of identical composition: $X_{AA} = 0.15$, $C_{nbisA} = 22$ mM.

The swelling degrees increase with the fraction of acrylic acid and decrease with the initial cross-linker concentration. The swelling equilibrium is determined by the balance between osmotic pressure and rubber elasticity. In cross-linked polyelectrolyte gels, the osmotic pressure is dominated by the translational entropy of the counterions. Thus, increasing acrylic acid concentration leads to an increase in the number of free counterions and, by consequence, the osmotic pressure. In turn, this results in larger swelling degrees. On the other hand, cross-linking increases the loss in conformational entropy upon swelling.

According to Flory, when the salt concentration in the surrounding solution is low compared to the concentration of fixed charges in the gel and the χ parameter satisfies $1/2 - \chi \leq 0.2$ (θ-conditions), the swelling degree Q scales with the concentration of fixed charges in the gel with an exponent of 3/2.[22] At higher ionic strength the exponent decreases to 6/5. Rubinstein et al. have developed a scaling theory of polyelectrolyte gels prepared by cross-linking of linear polymer chains.[23] They have expressed the equilibrium swelling degree Q as a function of the number of monomers A between effective charges and found $Q \sim A^{-3/2}$ and $Q \sim A^{-6/5}$ for the low- and high-salt regimes, respectively, under θ-conditions. This is essentially the same as Flory predicted since A is inversely proportional to the concentration of charged groups.[23]

While our gels fall into an intermediate regime between low and high salt concentrations, all three experimental curves exhibit scaling with the mole fraction of acrylic acid x_{AA} with exponents ranging from 0.22 at the highest and 0.36 at the lowest cross-link density. In all cases the exponents are therefore substantially less than unity, whereas scaling theory predicts the swelling degree to increase faster than proportionally with the charge density per monomer. Our data even suggest a tendency of the swelling degrees to saturate at high mole fraction of acrylic acid monomer, as can be seen by the systematic deviation from the power law fits in Figure 2. Similar findings have been reported by Kuhn et al. for poly(methacrylic acid) cross-linked with divinylbenzene.[24] They monitored the swelling degrees of the samples after addition of alkali, sufficient to neutralize a fraction α of acidic groups. While the equilibrium swelling degrees increased with the decrease of the cross-linking density, they also tend to reach some maximum constant

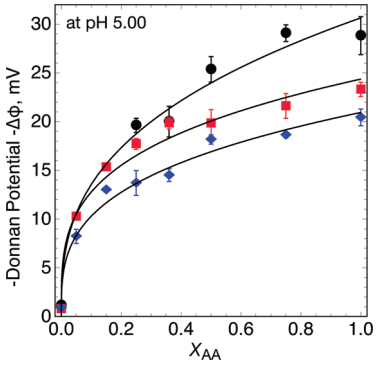

Figure 3. Donnan potential of PGs as a function of a fraction of acrylic acid monomer at preparation X_{AA} for different initial concentrations of the cross-linker nBisA C_{nbisA}: black circles, C_{nbisA} = 86 mM; red squares, C_{nbisA} = 43 mM; blue rhombs, C_{nbisA} = 22 mM. Potential values and the error bars represent the means and the standard deviations of data measured at three different positions on a sample (acquisition time t = 1 min, sampling interval 0.1 s).

values when degree of ionization α was larger than 0.4. Okay et al. also observed less than proportional increases in swelling for copolymers of acrylamide and 2-acrylamido-2-methylpropanesulfonic acid.[25]

Partially, this discrepancy may be attributed to the failure of the Gaussian approximation for the chain length distribution when the chains are highly extended, which is typically the case in highly swollen gels.[22] However, we suspect that the main cause lies in the actual ionization degree being a decreasing function of carboxylic acid group concentration at fixed pH. In other words, the effective pK_a of the acrylic acid groups is an increasing function of their concentration. It has been shown that the effective pK_a of poly(acrylic acid) increases from values around 4.25 at low dissociation to more than 6 at high degrees of dissociation.[26] In contact with a buffer at pH = 5, one would therefore expect the degree of dissociation to decrease with increasing spatial density of acrylic acid groups in the gel. This is corroborated by the fact that smaller scaling exponents correspond to the higher cross-linking degrees, i.e., higher concentrations of acrylic acid groups at equilibrium. A variable degree of ionization is also consistent with the observed nonlinear dependence of the Donnan potential on X_{AA}, as discussed below.

Donnan Potential. The equilibrium Donnan potential of the swollen gels from Figure 2 was determined as described above. The results are compiled in Figure 3. The polarity of the Donnan potential is negative, indicating a smaller concentration of positive ions in the gel than in the surrounding solution. The magnitude of the Donnan potential increases with both the acrylic acid concentration and the cross-link density. In pure acrylamide gels, the observed value is zero within experimental error, as expected due to the absence of ionizable groups, whereas pure acrylic acid gels at the highest cross-link density exhibit $\Delta\phi = -30$ mV. For a given cross-link density, the Donnan potential increases in magnitude with the acrylic acid content of the gels.

Similar results have been reported by Gulch et al.,[27] who obtained Donnan potential values for copolymers of acrylic acid and diallyldimethylammonium in the range −160 to −60 mV, while varying the concentration of the surrounding KCl solution. However, different compositions of our samples and different experimental conditions make our studies not directly comparable.

The surface of a polyelectrolyte gel can be considered as a semipermeable membrane, allowing only the counterions to pass into the surrounding liquid.[22] From this viewpoint, one would expect the Donnan potential to be purely a function of the number density of ionizable groups in the gel. Figure 4 shows the same data, plotted as a function of the molarity of ionizable groups (which reside on the acrylic acid moieties). This concentration has been calculated from the concentration of acrylic acid in the assay and the equilibrium swelling degree of each sample. The Donnan potential values collapse onto a single curve. A double-logarithmic plot (Figure 4) reveals that the data are well represented by a power law with an exponent of 0.4 ± 0.1. The fact that the observed exponent is significantly less than 1 suggests that at high acrylic acid concentrations not all ionizable groups are actually dissociated at pH 5. The acidity of the carboxlyic groups in poly(acrylic acid) has been shown to depend on the dissociation degree,[26] due to electrostatic interaction between the negative charges. This is reflected in the wide range of pK_a values of poly(acrylic acid) gels that have been reported, from as low as 4.25 up to 6.76.[21,28,29] The same effect appears to cause a dependence of the dissociation degree on the polymer density of gels containing poly(acrylic acid). Accurate modeling of the Donnan potential requires solving the Poisson−Boltzmann equation. However, a simple estimate can be obtained by assuming a functional shape of the ionic concentration profile across the surface of the gel with a width given by the Debye length. The total charge density $\rho(x)$ is given by the density of the counterions minus the density of the charges on the polymer backbone C_{fix}, which is assumed to follow a Heaviside function $H(x)$. We assume a $\tanh(x/\lambda)$ functional shape for the concentration profile of the counterions and obtain for the charge density

$$\rho(x) = C_{fix}\left(\frac{1}{1+e^{-x/\lambda}} - H(x)\right) \tag{3}$$

where x is a distance from gel−solution boundary. The Debye length λ is given by

$$\lambda = \sqrt{\frac{\varepsilon_0 \varepsilon_r k_B T}{2 N_A q^2 I}} \tag{4}$$

where ε_r and I denote the dielectric constant and ionic strength of the medium, respectively. The electric potential for a given charge distribution can be found by solving the Poisson equation

$$\nabla^2 \phi = -\frac{\rho}{\varepsilon_0 \varepsilon_r} \tag{5}$$

Integration of (5) with I = 0.1 M (corresponding to the buffer solution used in the experiments) and $C_{fix} = \alpha C_{AA}$, with a fixed dissociation degree α = 0.5 and concentration of dissociable unit C_{AA} = 0−0.5 M, leads to the Donnan potential represented as a dashed line in Figure 4. As it can be seen, there is good agreement between calculated and experimentally observed values for $C_{AA} < 0.15$ M. At higher concentrations, the observed Donnan potential is smaller than predicted, consistent with a decreasing degree of dissociation.

In order to directly relate the experimental values of the Donnan potential to the effective charge density, the pK_a values would need to be determined. Unfortunately, this is not a trivial experimental endeavor. While usually pK_a values of weak acids are obtained through potentiometric titration with a strong base, slow diffusion in polymer gels makes this impractical unless one works with gel microparticles. Another complication arises because the swelling

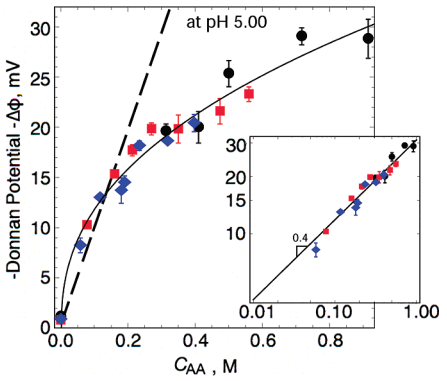

Figure 4. Dependence of the Donnan potential of PGs on acrylic acid concentration C_{AA} at a fully swollen state at pH 5.00 for different initial concentrations of the cross-linker nBisA C_{nbisA}: black circles, C_{nbisA} = 86 mM; red squares, C_{nbisA} = 43 mM; blue diamonds, C_{nbisA} = 22 mM. Potential values and the error bars represent the means and the standard deviations of data measured at three different positions on a sample (acquisition time t = 1 min, sampling interval 0.1 s). The dashed line represents the solution of Poisson equation for I = 0.1 M, C_{AA} = 0−0.5 M, and α = 0.5. Inset: double-logarithmic plot of the same data.

degree changes during titration, affecting in turn the pK_a of the AA groups.

Electromechanical Coupling. The mechanics problem of two nonconforming elastic half-spaces in contact was originally solved by Hertz.[30] To describe the geometry of our experiment, which involves a flat elastic sample being placed on a rigid substrate, we adopt a modification of the Hertzian solution developed for the indentation by a rigid solid of an elastic layer which is supported on arigid plane surface.[18] According to this model, the contact pressure distribution is described by eq 1 under the assumptions that the sample thickness $h \ll a$, and the elastic material is incompressible (Poisson ratio ν = 0.5). While in our case $h < a$, we find this modified Hertzian solution to provide a good description of our experimental data.

Assuming a linear relationship between potential and pressure $V(r) \sim kP(r)$, the potential distribution in the gel sample should have the same functional shape as the pressure given by eq 1. To avoid problems with static signal drift due to the input capacitance combined with the large input impedance of the signal acquisition system, the force applied to the sample was modulated as a square wave, and the resulting electric signals were recorded as a function of time. Application of the square-wave modulated force leads to a square-wave modulation of the contact pressure at any particular radial position inside of the contact circle and to an electric signal that correspondingly oscillates between minimum and maximum values. Figure 5A shows a typical example of the square-wave modulated recorded signal, together with its Fourier transform.

The change in potential response upon load application was recorded at different radial distances from the center with a resolution of 1 mm and digitally processed for the sequences of PGs. The Fourier transform (FT) of the signal reveals the amplitude of the response at the fundamental frequency f_0 = 0.025 Hz of the applied load (Figure 5). As the figure reveals, only the odd harmonics are present in the signal. Their amplitude ratios were found to correspond to the theoretical values to within better than 10%, demonstrating a linear relationship between the load and the voltage. The amplitude of a change in potential upon load application at a fundamental frequency f_0 = 0.025 Hz was calculated for all electrodes and plotted as a function of their radial position (Figure 6).

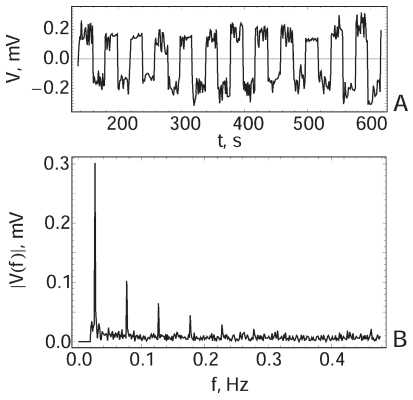

Figure 5. (A) Example of a typical recorded potential signal from an electrode. (B) Fourier transform of acquired potential signal after a digital band-pass filter (low cutoff: 0.02 Hz; high cutoff: 0.5 Hz) reveals an amplitude of a potential response at a fundamental frequency f_0 = 0.025 Hz. Acquired from PG with X_{AA} = 0.36, C_{nbisA} = 22 mM, and C_{AA} = 0.19 M at radial distance r = 1 mm.

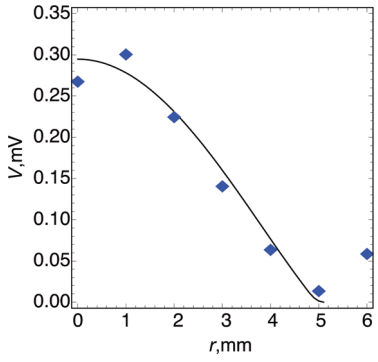

Figure 6. Example of radial distribution of potential response amplitudes. Each potential amplitude was determined from Fourier transform of an acquired square-wave potential signal. Solid curve represents pressure difference $\Delta P(r)$ calculated for known applied ΔF and contact radii a measured in an independent experiment. PG sample: C_{nbisA} = 22 mM, X_{AA} = 0.36, C_{AA} = 0.19 M.

The contact radii a were determined as described above in order to calculate the pressure difference $\Delta P(r)$ created in a sample resulting from the load change ΔF. This calculated pressure difference $\Delta P(r)$ was used to fit the experimentally measured radial potential distribution $\Delta V(r)$ (solid curve in Figure 6). The electromechanical coupling constant, defined as the proportionality coefficient between the pressure difference created in a sample and the potential difference measured $k = \Delta V(r)/\Delta P(r)$, was obtained as the sole fitting parameter. Figure 7 shows the variation of the electromechanical coupling constant k with a change in concentration of acrylic acid C_{AA} at a fully swollen state at pH 5.00, with error bars representing 90% confidence intervals. The coupling constant was found to be as large as 6 nV/Pa for the pure poly(acrylic acid) gel at the highest cross-link density (C_{nbisA} = 86 mM, X_{AA} = 1), and it decreased systematically, but not linearly, with the density of ionic groups in the sample — the data are well represented by $k \propto C_{AA}^{0.36}$. The potential amplitude for poly(acrylamide) gels at all cross-linking densities was below the experimental noise floor; therefore, the coupling constant k was taken equal to 0 for these cases.

While the data in Figure 7 exhibit a very clear trend, the agreement is not perfect. Two outlying data points are contained in Figure 7. We believe that these are either due to contact problems as a result of imperfect cleaning of the

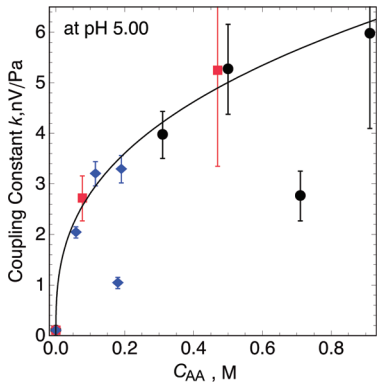

Figure 7. Variation of the electromechanical coupling constant $k = \Delta V/\Delta P$ with a change in concentration of acrylic acid C_{AA} at a fully swollen state at pH 5.00 for different initial concentrations of the cross-linker nBisA C_{nbisA}: black circles, $C_{nbisA} = 86$ mM; red squares, $C_{nbisA} = 43$ mM; blue rhombs, $C_{nbisA} = 22$ mM. Error bars represent 90% confidence intervals of the fit.

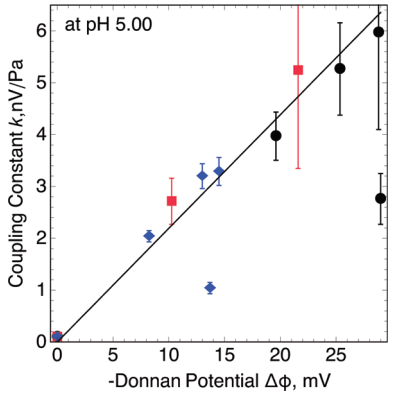

Figure 8. Electromechanical coupling constant $k = \Delta V/\Delta P$ versus Donnan potential measured at a fully swollen state at pH 5.00 for PGs with different initial concentrations of the cross-linker nBisA C_{nbisA}: black circles, $C_{nbisA} = 86$ mM; red squares, $C_{nbisA} = 43$ mM; blue rhombs, $C_{nbisA} = 22$ mM. Error bars represent 90% confidence intervals.

electrodes or due to mistakes in the assay of the preparation of these samples. Repetition of the same experiments with new samples produced data points close to the trend line. The quality of the fit exemplified in Figure 6 tended to be poorer for the samples with high concentration of acrylic acid, leading to increased error bars. We found this to be the result of increased deviation of the potential response from the predicted functional shape close to boundary of the contact circle.

An interesting finding emerges when the electromechanical coupling constant is plotted as a function of the Donnan potential (Figure 8): They are proportional to each other within experimental error. It is important to note that the data points in Figure 8 represent gels of widely different composition and cross-link densities. It appears that at least for the present class of materials, pH, and salinity, the coupling constant is directly related to the Donnan potential. The electromechanical coupling effect in these materials may therefore be understood simply as a pressure-induced modulation of the Donnan potential.

Conclusions

In this work, the relationship between the concentration of ionic groups in a soft polyelectrolyte gel (PG) and the electromechanical coupling constant has been studied by subjecting a sequence of PGs with different ionic charge densities to a well-defined pressure distribution, while monitoring the electrical potential response with a spatial resolution. PGs samples with a range of ionic charge densities in the equilibrated state were synthesized by copolymerization of acrylamide and acrylic acid at varying ratios, with different cross-link densities. The samples were characterized in terms of their equilibrium swelling degree in a buffer solution at pH 5 as well as in terms of their Donnan potential. Both exhibited a systematic variation with the density of ionizable groups in the gel, independent of whether that density was modulated through changes in acrylic acid content or by increased levels of cross-linking.

The results presented above demonstrate that indentation of flat samples while monitoring the potential response using an array of Pt electrodes is a practical and reproducible way of quantifying the electromechanical response of ionic polymer gels. The electromechanical coupling constant was found to vary systematically with the spatial density of the ionizable groups in the gel. To within experimental error, the coupling constant exhibited a proportional relationship to the Donnan potential. This suggests that the electromechanical response in soft ionic polymer gels can be understood simply as a pressure modulation of the Donnan potential.

Acknowledgment. We are indebted to Prof. M. R. Begley for originally suggesting indentation as a means to produce a well-defined spatial pressure distribution and to Prof. A. Dobrynin for helpful discussions. We also acknowledge Dr. J. Zhu for his help with preparation of Pt electrodes structure. This work was supported by the US National Science Foundation (DMR-0647790).

References and Notes

(1) Tanaka, T.; Nishio, I.; Sun, S.; Ueno-Nishio, S. *Science* **1982**, *218*, 467.
(2) Shahinpoor, M.; Bar-Cohen, Y.; Simpson, J. O.; Smith, J. *Smart Mater. Struct.* **1998**, *7*, R15–R30.
(3) Shahinpoor, M.; Kim, K. J. *Appl. Phys. Lett.* **2002**, *80*, 3445–3447.
(4) Nemat-Nasser, S. *J. Appl. Phys.* **2002**, 2889–2915.
(5) Beltran, S.; Baker, J.; Hooper, H.; Blanch, H.; Prausnitz, J. *Macromolecules* **1991**, *24*, 549–551.
(6) Doi, M.; Matsumoto, M.; Hirose, Y. *Macromolecules* **1992**, *25*, 5504–5511.
(7) de Gennes, P. G.; Okumura, K.; Shahinpoor, M.; Kim, K. J. *Europhys. Lett.* **2000**, *50*, 513–518.
(8) Beebe, D.; Moore, J.; Yu, Q.; Liu, R.; Kraft, M.; Jo, B.; Devadoss, C. *Proc. Natl. Acad. Sci. U.S.A.* **2000**, *97*, 13488.
(9) Beebe, D.; Moore, J.; Bauer, J.; Yu, Q.; Liu, R.; Devadoss, C.; Jo, B. *Nature* **2000**, *404*, 588–590.
(10) Cai, Q.; Grimes, C. *Sens. Actuators, B* **2001**, *79*, 144–149.
(11) De, S.; Aluru, N.; Johnson, B.; Crone, W.; Beebe, D.; Moore, J. *J. Microelectromech. Syst.* **2002**, *11*, 544–555.
(12) Yao, L.; Krause, S. *Macromolecules* **2003**, *36*, 2055–2065.
(13) Eddington, D.; Beebe, D. *J. Microelectromech. Syst.* **2004**, *13*, 586–593.
(14) Wallmersperger, T.; Kroplin, B.; Gulch, R. W. *Mech. Mater.* **2004**, *36*, 411–420.
(15) Yamaue, T.; Mukai, H.; Asaka, K.; Doi, M. *Macromolecules* **2005**, *38*, 1349–1356.
(16) Sawahata, K.; Gong, J. P.; Osada, Y. *Macromol. Rapid Commun.* **1995**, *16*, 713–716.
(17) Fiumefreddo, A.; Utz, M., manuscript in preparation.
(18) Johnson, K. *Contact Mechanics*; Cambridge University Press: Cambridge, 1987.
(19) Donnan, F. G. *Z. Phys. Chem.* (*Munich*) **1934**, *168*, 369–380.
(20) Cabaness, W. R.; Lin, T. Y. C.; Parkanyi, C. *J. Polym. Sci., Part A-1* **1971**, *9*, 2155–2162.
(21) Gong, P.; Wu, T.; Genzer, J.; Szleifer, I. *Macromolecules* **2007**, *40*, 8765–8773.
(22) Flory, P. *Principles of Polymer Chemistry*; Cornell University Press: Ithaca, NY, 1953.

(23) Rubinstein, M.; Colby, R.; Dobrynin, A.; Joanny, J. *Macromolecules* **1996**, *29*, 398–406.
(24) Kuhn, W.; Hargitay, B.; Katchalsky, A.; Eisenberg, H. *Nature* **1950**, *165*, 514–516.
(25) Okay, O.; Sariisik, S.; Zor, S. *J. Appl. Polym. Sci.* **1998**, *70*, 567–575.
(26) Tamura, T.; Uehara, H.; Ogawara, K.; Kawauchi, S.; Satoh, M.; Komiyama, J. *J. Polym. Sci., Part B: Polym. Phys.* **1999**, *37*, 1523–1531.
(27) Gulch, R.; Holdenriecf, J.; Weible, A.; Wallmersperger, T.; Kjoplin, B. *Smart Structures and Materials 2000: 6−8 March, 2000, Newport Beach, CA* **2000**, 193–202.
(28) Skouri, R.; Schosseler, F.; Munch, J.; Candau, S. *Macromolecules* **1995**, *28*, 197–210.
(29) Park, H.; Robinson, J. *Pharm. Res.* **1987**, *4*, 457–464.
(30) Hertz, H. *Verh. Ver. Beförderung Gewerbefleisses* **1882**, *61*, 449–462.